

# Gaze-guided Hand-Object Interaction Synthesis: Dataset and Method

Jie Tian, Ran Ji, Lingxiao Yang, Yuexin Ma, Lan Xu, Jingyi Yu, Ye Shi, Jingya Wang

ShanghaiTech University

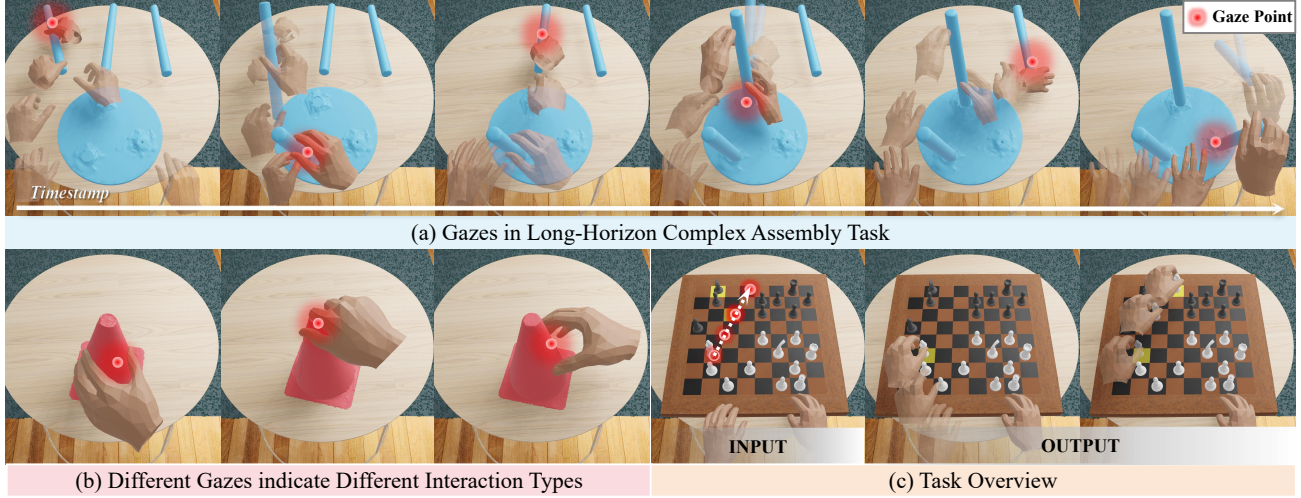


Figure 1. Gaze plays a crucial role in hand-object interaction tasks. The subfigure (a) illustrates how gaze helps coordinate the hands, objects, and brain during complex table assembly. The subfigure (b) shows how gaze affects attention allocation and grasp strategies. Building on these observations, we introduce the gaze-guided hand-object interaction synthesis task, as depicted in the subfigure (c), which uses gaze data as input to generate hand-object interactions that align with human intentions.

## Abstract

Gaze plays a crucial role in revealing human attention and intention, particularly in hand-object interaction scenarios, where it guides and synchronizes complex tasks that require precise coordination between the brain, hand, and object. Motivated by this, we introduce a novel task: Gaze-Guided Hand-Object Interaction Synthesis, with potential applications in augmented reality, virtual reality, and assistive technologies. To support this task, we present GazeHOI, the first dataset to capture simultaneous 3D modeling of gaze, hand, and object interactions. This task poses significant challenges due to the inherent sparsity and noise in gaze data, as well as the need for high consistency and physical plausibility in generating hand and object motions. To tackle these issues, we propose a stacked gaze-guided hand-object interaction diffusion model, named GHO-Diffusion. The stacked design effectively reduces the complexity of motion generation. We also introduce HOI-Manifold Guidance during the sampling stage of GHO-Diffusion, enabling fine-grained control over generated motions while maintaining the data manifold. Additionally, we propose a spatial-temporal gaze feature encoding for the diffusion condition and select diffusion results based on consistency scores between gaze-contact maps and gaze-interaction trajectories. Extensive experiments highlight the effectiveness of our method and the unique contributions of our dataset.

## Introduction

Gaze serves as a significant behavioral signal, directly reflecting human attention distribution and cognitive processes (Schneider 1995; Gottlieb et al. 2013; Desanghere and Marotta 2015). Extensive research has been conducted on gaze, including gaze estimation (Abdelrahman et al. 2023; Guan et al. 2023; Kothari et al. 2021; Fischer, Chang, and Demiris 2018) and human action prediction based on gaze (Kratzer et al. 2020; Zheng et al. 2022; DelPreto et al. 2022; Ragusa et al. 2021; Eren Akbiyik et al. 2023). While these studies have explored gaze in various applications, they have primarily focused on broad human motions, with limited attention given to hand movements and detailed dynamic interactions within fine-grained environments. Furthermore, gaze is particularly crucial in hand-object interactions, as it reveals “when, where, and how” the user interacts with the object. Figure 1(a) illustrates how gaze supports long-horizon synthesis for complex tasks, while Figure 1(b) shows that gaze indicates how humans interact with objects using different parts and interaction types. By effectively identifying objects and areas of focus, gaze enables the seamless integration of human intentions and motions, ensuring precise coordination and consistency between the brain, hands, and objects. This coordination is essential for executing complex interactions, such as grasping, manipulating, or positioning objects, thereby enhancing both the ef-

iciency and accuracy of these motions.

Motivated by this, we propose a novel task: Gaze-guided Hand-Object Interaction Synthesis, as shown in Figure 1(c). This task leverages gaze to naturally generate motions that align with human intent, eliminating the need for additional textual annotations or motion references. This approach is particularly well-suited for integration into VR/AR environments and assistive technologies. For example, in VR/AR settings, gaze-guided technology allows users to interact with virtual objects more intuitively by accurately predicting their intentions without the need for physical controllers. Additionally, it benefits individuals with disabilities by allowing them to control interactions through eye movements, enhancing their ability to express intentions and perform tasks

Existing hand-object datasets are limited to interactions between hands and objects, often neglecting gaze information. To fill this gap, we introduce GazeHOI, the first dataset that simultaneously integrates 3D modeling of gaze, hand, and object interactions. GazeHOI presents significant challenges due to the diverse shapes and sizes of objects, ranging from small items like chess pieces to larger, assemblable furniture. Additionally, the dataset covers a wide range of complex tasks, including repositioning objects, selecting specific targets within cluttered environments, organizing disordered items, and assembling furniture.

However, leveraging gaze data for generating hand and object motions presents significant challenges. The inherent sparsity and noise in gaze data make it difficult to reliably capture and interpret user intentions. Additionally, achieving high consistency and physical plausibility in the generated motions is a complex task, as it requires accurate synchronization between gaze input and corresponding hand-object interactions. To address these challenges, we propose a novel approach: a stacked gaze-guided hand-object interaction diffusion model, named GHO-Diffusion. We decouple the task into two stages: gaze-activated object dynamics synthesis and object-driven hand kinematic synthesis. Moreover, we introduce HOI-Manifold Guidance during the sampling stage of GHO-Diffusion. This technique allows for fine-grained control over the generated motions, ensuring they remain within the data manifold and adhere to the natural constraints of hand-object interactions. Additionally, to further leverage gaze information, we propose a spatial-temporal gaze feature encoding approach for the diffusion condition. This method captures both spatial and temporal aspects of gaze data, enhancing the diffusion process with detailed representations of gaze interactions. We also select diffusion results based on consistency scores between gaze-contact maps and gaze-interaction trajectories. Our contributions can be summarized as follows:

**1) A Novel Task and Dataset.** We introduce the novel task of gaze-guided hand-object interaction synthesis, which utilizes gaze to generate natural interaction motions that align with human intent. To support this task, we present GazeHOI, the first dataset incorporating gaze information for hand-object interactions.

**2) GHO-Diffusion Model.** We develop the Gaze-guided Hand-Object interaction Diffusion model, GHO-Diffusion,

which employs stacked diffusion models to reduce the complexity of motion modeling. Furthermore, we integrate the HOI-Manifold Guidance during the inference phase of GHO-Diffusion, providing fine-grained control over generated motions while maintaining the data distribution learned by the diffusion model.

**3) Gaze-Guided Feature Encoding and Motion Selection.**

We propose a gaze-guided spatial-temporal feature encoding as the diffusion condition, coupled with a mechanism to select diffusion results based on consistency scores between gaze-contact maps and gaze-interaction trajectories. This approach ensures that the generated motions are precisely aligned with the given gaze input.

## Related Work

### Gaze for Visual Perception

Gaze is fundamental to reveal intentional cues and offer insights into attention, interest, and cognitive processes. Due to the expense and accuracy limitations of gaze tracking equipment, the previous researchers have primarily explored methods for estimating gaze from a third-person perspective images or videos (Abdelrahman et al. 2023; Guan et al. 2023; Kothari et al. 2021; Fischer, Chang, and Demiris 2018). With the recent advancements in gaze tracking technology, acquiring accurate gaze information has become relatively more convenient, leading to the emergence of numerous datasets (Kratzer et al. 2020; Zheng et al. 2022; DelPreto et al. 2022; Ragusa et al. 2021; Eren Akbiyik et al. 2023) containing gaze annotations. Researchers have moved beyond solely acquiring gaze data and are now exploring methods for extracting rich information inherent in gaze, such as inferring the ego-trajectory of a driver’s vehicle (Eren Akbiyik et al. 2023) or predicting the interaction action labels (Liu et al. 2020). MoGaze and GIMO(Kratzer et al. 2020; Zheng et al. 2022) propose leveraging gaze to predict human motions within the scene, which reveals the potential of gaze in virtual reality (VR) and human-robot interaction scenarios. They solely focus on human motions, but fine-grained hand interaction generation is crucial for the realism of VR experiences. Therefore, in this work, we introduce the task of gaze-guided hand-object interaction motion synthesis.

### Hand-Object Interaction Dataset

Numerous datasets (Hampali et al. 2020; Chao et al. 2021; Kwon et al. 2021; Yang et al. 2022; Liu et al. 2022; Fan et al. 2023; Liu et al. 2024; Zhang et al. 2023; Zhao et al. 2023; Zhan et al. 2024) dedicated to hand-object interactions have been developed to facilitate the capture of hand and object poses and to deepen our understanding of these interactions, as shown in Table 1. Most datasets only capture simple interaction patterns, like grasping and moving, which is common but not comprehensive enough. HOI4D (Liu et al. 2022) and ARCTIC (Fan et al. 2023) explore the interaction of articulated objects. TACO (Liu et al. 2024) and Oakink2 (Zhan et al. 2024) captures scenes of simultaneous interactions with multiple objects. Furthermore, existing datasets focus exclusively on the relationship between hands and objects, neglecting the role of gaze. To address this gap, we

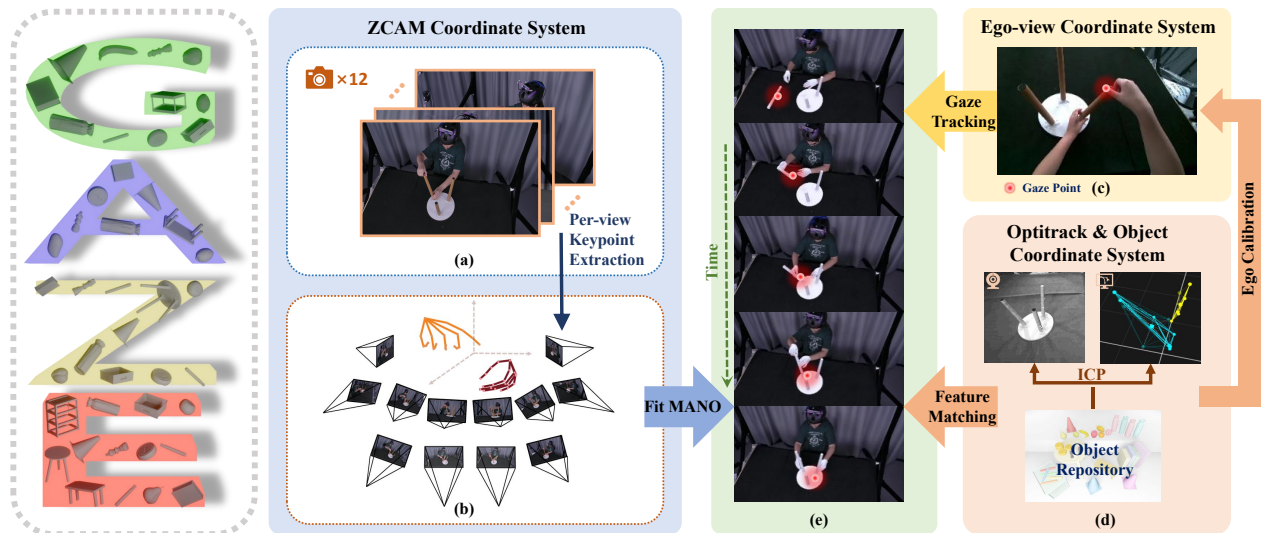


Figure 2: Automatic data processing pipeline. (a) displays 12-view images from the raw video. (b) uses mediapipe(Lugaresi et al. 2019) to get hand 2D joints and triangulation to obtain the 3D joints. (c) shows the ego view with a gaze point. (d) illustrates the objects acquired by the scanner and the marker tracking process. (e) shows the result of hand-object motion.

	Gaze	Ego	Multi-obj	Complex	#views	#images
HO-3D (Hampali et al. 2020)	×	×	×	×	1-4	78K
DexYCB (Chao et al. 2021)	×	×	×	×	8	582K
H2O (Kwon et al. 2021)	×	✓	×	×	5	571K
OakInk (Yang et al. 2022)	×	×	×	×	4	230K
HOI4D (Liu et al. 2022)	×	✓	×	×	2	2.4M
ARCTIC (Fan et al. 2023)	×	✓	×	×	9	2.1M
TACO (Liu et al. 2024)	×	✓	✓	✓	13	5.2M
OAKINK2 (Zhan et al. 2024)	×	✓	✓	✓	4	4.01M
<b>GazeHOI</b>	✓	✓	✓	✓	13	3.2M

Table 1: Comparison of GazeHOI with existing 4D hand-object interaction datasets.

introduce a comprehensive egocentric dataset enriched with detailed gaze annotations. This dataset captures the dynamics of hand-object interactions across a wide range of tasks, from arranging chess pieces to assembling furniture — scenarios not covered in existing datasets. Our goal is to bridge the shortcomings of current datasets by providing a resource that reflects the complexity of real-world interactions and emphasizes the importance of gaze in predicting human intent and managing multi-object manipulation.

### Hand-Object Motion Synthesis

In the field of hand-object motion synthesis, prior efforts have mainly centered on frame-wise generation (Li et al. 2022; Jiang et al. 2021; Liu et al. 2023; Grady et al. 2021). For dynamic hand-object interaction, previous methods typically rely on motion references, such as trajectories (Zhang et al. 2021; Karunratanakul et al. 2023; Taheri et al. 2024; Zhou et al. 2024; Li, Wu, and Liu 2023; Zheng et al. 2023) or grasp references (Christen et al. 2022), or only focus on approaching stage (Taheri et al. 2022; Ghosh et al. 2023). Recently, there are several works that study the hand-object interaction generation directly based on text (Cha et al. 2024; Christen et al. 2024), significantly reducing the reliance on

specific conditions. Building on advancements in 3D gaze acquisition technology, our work further relaxes these constraints by generating hand-object interactions directly from gaze data. Compared to text, gaze-based generation aligns more closely with the user’s intent, resulting in more intuitive hand-object interactions.

### GazeHOI Dataset

Existing datasets primarily focus on the interaction between hands and objects, overlooking the crucial role of gaze. However, a comprehensive understanding of interaction requires coordinated hand-eye-object cooperation. To address this gap, we present GazeHOI, the first interaction dataset that simultaneously incorporates 3D modeling of gaze, hand, and object interactions. GazeHOI encompasses 237K frames with an average duration of 19.1 seconds and 2-4 objects per sequence, further divisible into 1378 subsequences. We collect 33 different objects with various shape and size, the smallest of which is a chess piece with a height of 7cm and a mere diameter of 2cm. Each sequence is accompanied by a task-level description, which varies in complexity, and includes repositioning objects to another location, selecting specific targets from cluttered environments, organizing items from disarray into order, and assembling furniture. This rich variety aims to provide comprehensive insights into the intricate dynamics of interactive behaviors.

### Data Collection

We recruited 10 volunteers (5 males and 5 females) to assist us in data collection. Before the collection process, we provided the participants with a comprehensive script that detailed the tasks they were required to complete. For each task, participants were asked to perform multiple iterations. Consequently, individuals often scan their surroundings to gain a preliminary understanding of the environment before

executing the action in unfamiliar settings, leading to longer gaze duration for task-relevant objects. As familiarity with the scene increases, the gaze becomes more focused, and the gaze duration correspondingly decreases. This approach ensures the authenticity and naturalness of the gaze data, accurately reflecting real-world gaze behavior.

## Data Annotation

**3D Hand Pose.** 12 synchronized ZCAM cameras afford us an exhaustive 3D perspective of the hand, as shown in Figure 2(a). By harnessing the capabilities of MediaPipe (Lugaresi et al. 2019), we execute 2D hand keypoint tracking across individual video frames. Through the application of triangulation algorithms, we transition the 2D keypoints observed from disparate views to their respective 3D coordinates in global space shown in Figure 2(b). Subsequently, we derive the corresponding MANO (Romero, Tzionas, and Black 2017) parameters through an optimization process that accounts for joint alignment, realistic anatomical constraints.

**Object 6D Pose.** We focus on rigid objects, enabling us to determine the 6D poses by tracking reflective markers attached to the surfaces via Optitrack. We strategically placed at least eight 3mm markers on each object to minimize interference with natural interactions and prevent occlusions that could affect marker recognition. Before data collection, we employ a 3D scanner to capture the precise geometry of the object surfaces. The Iterative Closest Point algorithm is used to convert the reflection points detected by OptiTrack into the 6D pose of the object. Figure 2(d) shows our object repository acquired by scanner and tracking process.

**Gaze Acquisition.** The eye tracker Pupil Core provides 3D gaze data from an egocentric viewpoint, requiring us to perform ego calibration to unify gaze, hand, and object data within a single coordinate system. Similar to object tracking, we attach markers to the ego camera to achieve this calibration. We also apply post-processing techniques, such as removing gaze data with very short durations and smoothing, to reduce noise and enhance the quality of the gaze data. Figure 2(c) shows the gaze during data collection.

## Method

### Problem Definition

We define a gaze-consistent hand-object interaction sequence of length  $l$  as  $\mathbf{S} = \langle \mathbf{G}, \mathbf{H}, \mathbf{O} \rangle$ , where  $\mathbf{G} = \{\mathbf{g}_i\}_{i=1}^l$  represents the gaze sequence, with each  $\mathbf{g}_i \in \mathbb{R}^3$  denoting the gaze point in the  $i$ -th frame.  $\mathbf{H} = \{\mathbf{h}_l^i, \mathbf{h}_r^i\}_{i=1}^l$  denotes the hand motion sequences, comprising left-hand motions  $\mathbf{h}_l^i$  and right-hand motions  $\mathbf{h}_r^i$ . Each hand motion  $\mathbf{h}^i = \{\mathbf{R}_h^i, \mathbf{T}_h^i, \theta^i, \beta\} \in \mathbb{R}^{61}$  follows the MANO (Romero, Tzionas, and Black 2017) parameterization, where  $\mathbf{R}_h^i$  is the rotation,  $\mathbf{T}_h^i$  is the translation,  $\theta^i$  represents the pose and  $\beta$  represents shape parameters;  $\mathbf{O} = \{\mathbf{o}^i\}_{i=1}^l$  is the object motion sequence, where each  $\mathbf{o}^i = \{\mathbf{R}_o^i, \mathbf{T}_o^i\} \in \mathbb{SE}(3)$  denotes the object’s pose, with  $\mathbf{R}_o^i$  as the rotation and  $\mathbf{T}_o^i$  as the translation. Additionally, we define the object geometry as a set of vertices  $\mathbf{P}_o = \{\mathbf{p}_o^n\}_{n=1}^N \in \mathbb{R}^{N \times 3}$ , where  $N$  represents the number of object vertices. Given the input

$\mathcal{I} = \{\mathbf{G}, \mathbf{h}_l^1, \mathbf{h}_r^1, \mathbf{o}^1, \mathbf{P}_o\}$ , our objective is to derive a subsequent hand-object interaction sequence  $\langle \mathbf{H}, \mathbf{O} \rangle$  that is not only consistent with the gaze but also exhibits natural and realistic interactions between the hand and the object.

### GHO-Diffusion: Gaze-guided Hand-Object Diffusion

GHO-Diffusion decouples the complex hand-object interaction into two stacked diffusion stages, Object Dynamics Synthesis with Spatial-Temporal Gaze Encoding and Hand Kinematic Synthesis with HOI-Manifold Guidance as shown in Figure 3(a). This decoupling strategy reduces modeling complexity while effectively capturing both global spatial-temporal positioning and the intricate details of hand-object interaction motions.

The diffusion model contains a fixed forward process  $q(\mathbf{x}_t|\mathbf{x}_0) = \mathcal{N}(\sqrt{\alpha_t}\mathbf{x}_0, (1 - \alpha_t)\mathbf{I})$  which gradually adds Gaussian noise to clean data  $\mathbf{x}_0$  until it becomes pure noise  $\epsilon \sim \mathcal{N}(\mathbf{0}, \mathbf{I})$  and train a denoiser  $p_\theta(\mathbf{x}_t, t, \mathbf{c})$  to gradually denoise  $\mathbf{x}_T \sim \mathcal{N}(\mathbf{0}, \mathbf{I})$  to generate  $\mathbf{x}_0$  in the reverse process. Instead of predicting  $\epsilon_t$  at each time step  $t$ , we follow MDM (Tevet et al. 2022) to predict  $\hat{\mathbf{x}}_0$  and optimizing  $p_\theta(\mathbf{x}_t, t, \mathbf{c})$  using the simple objective function:

$$\mathcal{L}_{\text{simple}} = \mathbb{E}_{\mathbf{x}_0 \sim q(\mathbf{x}_0|\mathbf{c}), t \sim [1, T]} \|\mathbf{x}_0 - p_\theta(\mathbf{x}_t, t, \mathbf{c})\|_2^2. \quad (1)$$

### Stage-1: Object Dynamics Synthesis with Spatial-Temporal Gaze Encoding.

The gaze point locations are closely related to the object surface vertices, and since object motions have fewer degrees of freedom compared to hand motions, so we generate the object motions first. Gaze is a sparse and noisy signal, making it challenging to encode effectively. Drawing inspiration from GIMO (Zheng et al. 2022), we design a gaze-guided spatial-temporal feature encoding module for object diffusion. We define  $\mathbf{f}_o^k$  as the  $k$ -th local per-point object spatial feature extracted by PointNet++ (Qi et al. 2017). Then according to the spatial relationship between gaze and object points, we can calculate gaze spatial feature:

$$\mathbf{f}_g = \|\mathbf{G} - \mathbf{P}_o^{k^*}\|^{-1} \mathbf{f}_o^{k^*}, \quad (2)$$

where  $k^* = \arg \min_{k=1}^N \|\mathbf{G} - \mathbf{P}_o^k\|$ , representing the index of the object points that is closest to the gaze point in  $i$ -th frame. Subsequently, these spatial features are processed through a self-attention mechanism to extract the final spatial-temporal condition features:

$$\mathbf{c}_g = \text{softmax} \left( \frac{\mathbf{f}_g \mathbf{W}_Q (\mathbf{f}_g \mathbf{W}_K)^\top}{\sqrt{d}} \right) \mathbf{f}_g \mathbf{W}_V, \quad (3)$$

where  $\mathbf{W}_Q$ ,  $\mathbf{W}_K$ , and  $\mathbf{W}_V$  are trainable weight matrices, and  $d$  is the dimension of the feature. We leverage the gaze spatial-temporal features  $\mathbf{c}_g$ , along with the object geometry  $\mathbf{P}$  and initial object pose  $\mathbf{o}^1$  as stage-1 diffusion condition and employ the objective function in Equation 4 as Stage-1 training loss to generate object motions  $\hat{\mathbf{O}}$ :

$$\mathcal{L}_{\text{stage1}} = \lambda_\alpha \mathcal{L}_{\text{simple}} + \lambda_v \mathcal{L}_{\text{verts}} + \lambda_t \mathcal{L}_{\text{trans}} + \lambda_s \mathcal{L}_{\text{smooth}}. \quad (4)$$

where  $\mathcal{L}_{\text{simple}}$  is defined by Equation 1,  $\mathcal{L}_{\text{trans}}$  indicates object translation loss, while  $\mathcal{L}_{\text{verts}}$  represents object vertices loss. The details of these loss terms are provided in the Appendix.

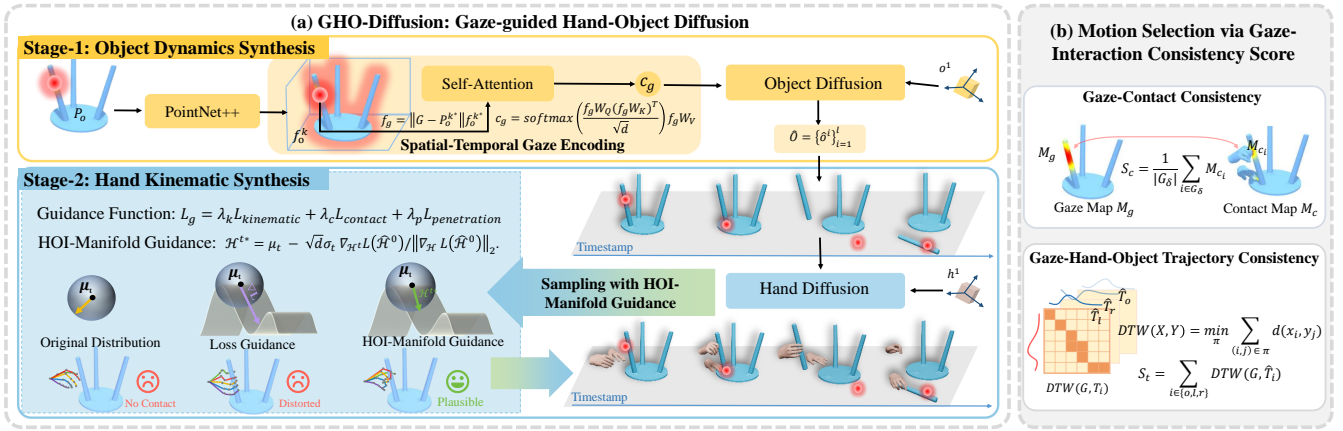


Figure 3: Pipeline overview. The subfigure (a) illustrates the stacked framework of the gaze-guided hand-object interaction diffusion model, GHO-Diffusion. The subfigure (b) shows the gaze-interaction consistency score for motion selection.

### Stage-2: Hand Kinematic Synthesis with HOI Guidance

In this stage, we leverage the object motions  $\hat{O}$  generated in Stage-1 to synthesize the corresponding hand motions  $\hat{H}$  through a hand diffusion process. Hand motion synthesis presents greater complexity compared to object motion synthesis, primarily because hand movements are highly articulated and require more stringent constraints to ensure natural and physically plausible outcomes. To address this, we adopt a canonicalized hand-object interaction representation:  $\mathcal{H} = [\mathbf{J}, \mathbf{C}, \mathbf{F}, \mathbf{v}, \mathbf{a}]$ . Here, hand poses are represented by joint positions  $\mathbf{J}$ , as neural networks typically learn translations more effectively than rotations. The contact flag  $\mathbf{C} \in \mathbb{R}^{42}$  encodes the contact status of each joint, while the offset vector  $\mathbf{F}$  represents both hand-object and inter-hand spatial displacements. The velocity vector  $\mathbf{v}$  captures both linear and angular velocities for each hand, including their relative velocities, and the acceleration vector  $\mathbf{a}$  is similarly defined. To generate the hand motions  $\hat{H}$ , we condition the synthesis on the generated object motions  $\hat{O}$ , alongside object geometry  $\mathbf{P}$  and the initial hand pose  $\mathbf{h}^1$  in Stage-2. For training, we employ the objective function from Equation 1 and introduce a bone length loss  $\mathcal{L}_{\text{bone}}$  to maintain the structural integrity of the hand:

$$\mathcal{L}_{\text{stage2}} = \lambda_\beta \mathcal{L}_{\text{simple}} + \lambda_b \mathcal{L}_{\text{bone}}. \quad (5)$$

Since the hand diffusion effectively captures the overall distribution of hand-object interactions, it falls short of achieving precision in finer details, such as maintaining contact or avoiding penetrations. Therefore, we introduce HOI-Manifold Guidance to strengthen the physics constraint while preserving the original data distribution. We define three guidance functions from the perspective of Kinematic, Contact and Penetration.

**(1) Hand-Object Kinematic Guidance.** We define redundancy parameters to enhance the reliability of hand motions while using only the hand joints for subsequent steps. The kinematic consistency guidance is designed for test-time adaptation, ensuring that the generated parameters remain consistent with those recalculated from the generated hand

joints and object motion conditions. The loss function is as follow,

$$\mathcal{L}_{\text{kinematic}} = \|\hat{\mathbf{F}} - \tilde{\mathbf{F}}\|_2 + \|\hat{\mathbf{v}} - \tilde{\mathbf{v}}\|_2 + \|\hat{\mathbf{a}} - \tilde{\mathbf{a}}\|_2. \quad (6)$$

**(2) Hand-Object Contact Guidance.** We define a contact loss to minimize the distance between hand joints that are near the object’s surface but not yet in contact:

$$\mathcal{L}_{\text{contact}} = \frac{\sum_{i=1}^l d(\hat{\mathbf{J}}^i, \mathbf{P}_o^i) \cdot \mathbb{I}(d(\hat{\mathbf{J}}^i, \mathbf{P}_o^i) < \tau)}{\sum_{i=1}^l \mathbb{I}(d(\hat{\mathbf{J}}^i, \mathbf{P}_o^i) < \tau) + \epsilon}, \quad (7)$$

where  $d(\hat{\mathbf{J}}^i, \mathbf{P}_o^i)$  is the closest distance between hand joint  $\hat{\mathbf{J}}^i$  and object surface  $\mathbf{P}_o^i$  in  $i$ -th frame,  $\tau$  is the contact threshold,  $\mathbb{I}$  is the indicator function, and  $\epsilon$  is a small constant to prevent division by zero.

**(3) Hand-Object Penetration Guidance.** We calculate the dot product between the hand-object offset and the object surface normal to measure the penetration as follows,

$$\mathcal{L}_{\text{penetration}} = - \sum_{i=1}^l \min(0, \tilde{\mathbf{F}}^i \cdot \mathbf{n}^i + \eta), \quad (8)$$

where  $\tilde{\mathbf{F}}^i$  is the recalculated offset vector from the generated hand joint  $\hat{\mathbf{J}}^i$  to the object surface  $\mathbf{P}_o^i$  in  $i$ -th frame,  $\mathbf{n}^i$  is the normal vector at the closest object point in  $i$ -th frame, and  $\eta$  is a small constant that defines the acceptable penetration threshold. The overall guidance loss function is

$$\mathcal{L}_g = \lambda_k \mathcal{L}_{\text{kinematic}} + \lambda_c \mathcal{L}_{\text{contact}} + \lambda_p \mathcal{L}_{\text{penetration}}. \quad (9)$$

The naive guidance strategy, which directly adds the computed gradient  $\nabla_{\mathcal{H}^t} \mathcal{L}(\hat{\mathcal{H}}^0)$  to the sample, may misalign the final motions with the original data distribution, resulting in unnatural motions. Therefore, we aim to develop a guidance strategy that can achieve guidance targets while preserving the original distribution. Recently, a conditional diffusion model with the Spherical Gaussian constraint, named DSG (Yang et al. 2024) is proposed to offer larger, adaptive step sizes while preserving the original data distribution. However, its effectiveness has mainly been shown

in image-generation tasks. Motivated by DSG, we introduce the Spherical Gaussian constraint to our sampling process, which ensures that the generated hand motion remains within the clean data distribution, resulting in natural and smooth hand motion generation.

We utilize closed-form solution  $\mathcal{H}^{t*}$  that enforces sampling in gradient descent direction while preserving  $\mathcal{H}^{t*}$  within noisy data distribution. This can ensure the generated  $\mathcal{H}^0$  remaining within the clean data manifold:

$$\mathcal{H}^{t*} = \mu_t - \sqrt{d}\sigma_t \nabla_{\mathcal{H}^t} \mathcal{L}_g(\hat{\mathcal{H}}^0) / \|\nabla_{\mathcal{H}^t} \mathcal{L}_g(\hat{\mathcal{H}}^0)\|_2, \quad (10)$$

where  $\sigma_t$  represents the variance in time step  $t$  and  $d$  represents the data dimensions. To enhance generation diversity, we re-weight the direction of  $\mathcal{H}^{t*}$  and the sampling point  $\mathcal{H}^t$  similar to Classifier-free guidance:

$$\mathbf{D} = \mathcal{H}^{t*} + w(\mathcal{H}^{t*} - \mathcal{H}^t), \quad (11)$$

$$\mathcal{H}^t = \mu_t + \sqrt{d}\sigma_t \mathbf{D} / \|\mathbf{D}\|, \quad (12)$$

where  $w$  represents the guidance rate that lies in  $[0,1]$  and  $\mathbf{D}$  represents the weighted direction. After sampling, we use post-optimization to get the corresponding MANO parameters  $\hat{\mathbf{H}}$ . Details are illustrated in the Appendix.

### Motion Selection via Gaze-Interaction Consistency Score

Motions generated by diffusion do not always fully conform to the gaze distribution. To address this, we explore gaze-interaction consistency from both a local and a global perspective, as shown in Figure 3(b). Locally, inspired by De-sanghere and Marotta (2015), we observe that areas receiving more visual attention are more likely to be contacted. So we compute the contact map  $\mathbf{M}_c = e^{-\alpha \cdot d(\mathbf{P}_h, \mathbf{P}_o)}$  and gaze map  $\mathbf{M}_g = e^{-\alpha \cdot d(\mathbf{G}, \mathbf{P}_o)}$  separately by the distance from hand vertices  $\mathbf{P}_h$  and gaze point  $\mathbf{G}$  to the object surface  $\mathbf{P}_o$ . The gaze-contact consistency score  $S_c$  is then calculated as follows,

$$S_c = \frac{1}{|\mathbf{G}_\delta|} \sum_{i \in \mathbf{G}_\delta} \mathbf{M}_{c_i}, \quad (13)$$

where  $\mathbf{G}_\delta$  is the set of object points index that indicates where the distance  $d(\mathbf{G}, \mathbf{P}_o) < \delta$ , and  $|\mathbf{G}_\delta|$  is the number of elements in this set. Globally, gaze-hand-object trajectories are expected to exhibit inherent relationships. To quantify this, we use Dynamic Time Warping (DTW) (Seshan 2022) to measure the gaze-hand-object trajectory similarity,

$$\text{DTW}(\mathbf{X}, \mathbf{Y}) = \min_{\pi} \sum_{(i,j) \in \pi} d(x_i, y_j), \quad (14)$$

where  $\pi$  is a warping path that aligns  $\mathbf{X}$  and  $\mathbf{Y}$ , and  $d(x_i, y_j)$  is the distance between points  $x_i$  and  $y_j$ . The gaze-hand-object trajectory consistency score  $S_t$  is then defined as:

$$S_t = \text{DTW}(\mathbf{G}, \hat{\mathbf{T}}_l) + \text{DTW}(\mathbf{G}, \hat{\mathbf{T}}_r) + \text{DTW}(\mathbf{G}, \hat{\mathbf{T}}_o). \quad (15)$$

Then we combine  $S_c$  and  $S_t$  to select the top-k motions  $(\hat{\mathbf{H}}, \hat{\mathbf{O}})$  that are most consistent with the gaze signals.

## Experiments

### Data Split and Evaluation Metrics

We divided 1378 sequences into a training set with 1103 sequences and a test set comprising 275 sequences. To mitigate the model’s potential overfitting to object-specific traits, the test set exclusively includes objects not represented in the training set. Our evaluation metrics includes three parts: 1) motion consistency with gaze and accuracy by evaluating the hand Mean Per Joint Position Error (MPJPE), object Mean Per Vertex Position Error (MPVPE), and the Final Object Location (FOL); 2) the stability and realism of hand-object interactions using the Contact Frame radio (CF) and the Penetration Depth (PD); 3) some basic generation metrics, including FID and Diversity. The FID quantifies the dissimilarity between the real and generated motions, while the diversity measures the variance of different motions. Additionally, we conduct a user study in which participants rated the gaze-motion consistency (GMC) and the interactions naturalness (IN) on a five-point scale. Higher scores reflect better motion generation quality.

### Comparison

Our method is the first to generate both hand and object motions from gaze data, and there are no direct methods available for comparison. The most closely related state-of-the-art work is Text2HOI (Cha et al. 2024), which generates a contact map conditioned on texts and then combines it to produce hand-object motions. We found that the gaze map and contact map are consistent, allowing us to adapt this approach by generating the contact map conditioned on gaze. We also employed MDM (Tevet et al. 2022) as a baseline, as it is a classic benchmark for diffusion-based motion generation. To better extract gaze features and for a fairer comparison, both MDM and Text2HOI use our designed spatial-temporal gaze encoding. Additionally, Object-Conditioned Hand Motion Synthesis is a key component of our method. Although there is no direct baseline for our entire task, OMOMO (Li, Wu, and Liu 2023) is closely related to this aspect, so we compare our approach with OMOMO, using our fully designed stage-1 to acquire the object motions. Quantitative and qualitative results are shown in Table 2 and Figure 4, demonstrating that our method significantly outperforms the other baselines.

### Ablation Study

#### Results on Seen and Unseen Objects.

As shown in Figure 4, our method outperforms others on both seen and unseen objects, delivering motions that are natural and plausible, while closely aligning with the underlying information encoded in the gaze data. A more detailed quantitative comparison will be provided in the Appendix.

**Gaze Representation and Encoding.** As the first method to use gaze as a condition for motion generation, we explore the effectiveness of different gaze representations and spatial-temporal feature encoding. The results are in Table 3. The results show that our method effectively captures both spatial and temporal features, enabling efficient extraction of the rich information encoded in gaze data.

Methods	Accuracy			Grasp Quality		Generation		Human Perception	
	MPVPE ↓	FOL ↓	MPJPE ↓	CF ↑	PD ↓	FID ↓	Diversity ↑	GMC ↑	IN ↑
MDM*	146.8	228.0	166.6	62.55	2.52	0.071	4.174	3.70	3.40
Text2HOI*	325.0	327.1	258.1	59.64	2.51	0.719	4.188	2.95	2.50
OMOMO*	-	-	161.2	62.61	2.49	0.051	4.121	4.15	4.05
<b>Ours</b>	<b>117.4</b>	<b>146.5</b>	<b>144.8</b>	<b>68.10</b>	<b>2.46</b>	<b>0.044</b>	<b>4.217</b>	<b>4.75</b>	<b>4.60</b>

Table 2: Quantitative comparison between baselines and our method. \* indicates an adapted version of the original method tailored to our task. - refers to the same results as Ours, as OMOMO uses the same Stage-1 module to acquire object motions. The ground truth Diversity is 4.227 and diversity results are better if the metric is closer to the real distribution.

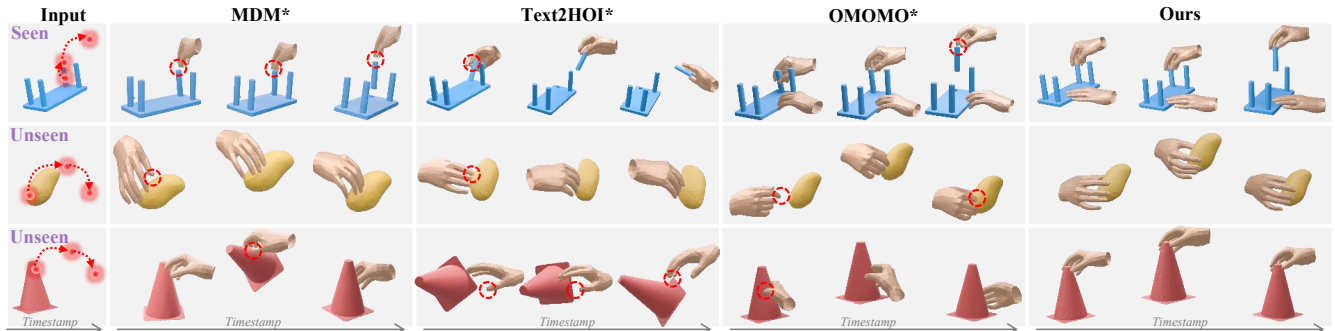


Figure 4: Qualitative results between baseline methods and our method.

	MPVPE ↓	FOL ↓	GMC ↑
gaze ray	126.7	189.2	3.95
w/o spatial	128.4	193.8	3.90
w/o temporal	119.3	163.4	4.15
<b>Ours-</b>	<b>117.9</b>	<b>157.6</b>	<b>4.25</b>

Table 3: Ablation on Gaze Representation and Encoding. Ours- means our full method without motion selection for a fair comparison.

**HOI-Manifold Guidance.** The guidance-free method suffers from problems like lack of contact and penetration, while the naïve guidance strategy partially mitigates these problems but introduces motion distortions, compromising the naturalness of the results. In contrast, our HOI-Manifold Guidance strategy strikes a balance between these challenges, achieving superior outcomes as shown in Table 4.

	MPJPE ↓	CF ↑	PD ↓	IN ↑
w/o guidance	155.3	64.65	2.61	3.9
naïve guidance	156.8	63.66	<b>2.44</b>	3.5
<b>Ours-</b>	<b>154.3</b>	<b>65.77</b>	2.51	<b>4.45</b>

Table 4: Ablation on Different Guidance Strategies. Ours- means our full method without motion selection for a fair comparison.

**Motion Selection via Gaze-interaction Consistency Score.** Table 5 demonstrates the effectiveness of our designed gaze-interaction consistency score, showing that motions selected by this score are more closely aligned with the

information implied in the gaze data.

	MPVPE ↓	FOL ↓	MPJPE ↓	GMC ↑
w/o select	117.9	157.6	154.3	4.25
w/o global	117.9	156.4	145.7	4.40
w/o local	117.5	148.9	149.8	4.35
<b>Ours</b>	<b>117.4</b>	<b>146.5</b>	<b>144.8</b>	<b>4.75</b>

Table 5: Ablation on Motion Selection via Gaze-interaction Consistency Score.

## Conclusion

We have proposed a novel task of Gaze-guided Hand-Object Interaction Synthesis and introduced a new dataset GazeHOI to support this task. GazeHOI is the first dataset to capture simultaneous 3D modeling of gaze, hand, and object interactions. To address this task, we proposed a stacked gaze-guided hand-object interaction diffusion model, named GHO-Diffusion, and further introduced HOI-Manifold Guidance in the sampling stage to force the guidance within the data manifold. We further exploited the consistency between gaze-contact maps and gaze-interaction trajectories to refine the generated motions. The extensive experimental results have validated the effectiveness of our method and the unique contributions of our dataset. While GazeHOI captures a diverse range of objects and tasks, it does not include articulated objects, which could present unique interaction challenges. In future work, we aim to extend this research by incorporating additional modalities, such as text descriptions and electromyography data to generate more context-aware interactive motions.

## References

- Abdelrahman, A. A.; Hempel, T.; Khalifa, A.; Al-Hamadi, A.; and Dinges, L. 2023. L2cs-net: Fine-grained gaze estimation in unconstrained environments. In *2023 8th International Conference on Frontiers of Signal Processing (ICFSP)*, 98–102. IEEE.
- Cha, J.; Kim, J.; Yoon, J. S.; and Baek, S. 2024. Text2HOI: Text-guided 3D Motion Generation for Hand-Object Interaction. In *Proceedings of the IEEE/CVF Conference on Computer Vision and Pattern Recognition*, 1577–1585.
- Chao, Y.-W.; Yang, W.; Xiang, Y.; Molchanov, P.; Handa, A.; Tremblay, J.; Narang, Y. S.; Van Wyk, K.; Iqbal, U.; Birchfield, S.; Kautz, J.; and Fox, D. 2021. DexYCB: A Benchmark for Capturing Hand Grasping of Objects. In *Proceedings of the IEEE/CVF Conference on Computer Vision and Pattern Recognition (CVPR)*, 9044–9053.
- Christen, S.; Hampali, S.; Sener, F.; Remelli, E.; Hodan, T.; Sauser, E.; Ma, S.; and Tekin, B. 2024. Diffh2o: Diffusion-based synthesis of hand-object interactions from textual descriptions. *arXiv preprint arXiv:2403.17827*.
- Christen, S.; Kocabas, M.; Aksan, E.; Hwangbo, J.; Song, J.; and Hilliges, O. 2022. D-grasp: Physically plausible dynamic grasp synthesis for hand-object interactions. In *Proceedings of the IEEE/CVF Conference on Computer Vision and Pattern Recognition*, 20577–20586.
- DelPreto, J.; Liu, C.; Luo, Y.; Foshey, M.; Li, Y.; Torralba, A.; Matusik, W.; and Rus, D. 2022. ActionSense: A multimodal dataset and recording framework for human activities using wearable sensors in a kitchen environment. *Advances in Neural Information Processing Systems*, 35: 13800–13813.
- Desanghere, L.; and Marotta, J. J. 2015. The influence of object shape and center of mass on grasp and gaze. *Frontiers in psychology*, 6: 1537.
- Eren Akbiyik, M.; Savov, N.; Pani Paudel, D.; Popovic, N.; Vater, C.; Hilliges, O.; Van Gool, L.; and Wang, X. 2023. G-MEMP: Gaze-Enhanced Multimodal Ego-Motion Prediction in Driving. *arXiv e-prints*, arXiv–2312.
- Fan, Z.; Taheri, O.; Tzionas, D.; Kocabas, M.; Kaufmann, M.; Black, M. J.; and Hilliges, O. 2023. ARCTIC: A Dataset for Dexterous Bimanual Hand-Object Manipulation. In *Proceedings of the IEEE/CVF Conference on Computer Vision and Pattern Recognition (CVPR)*, 12943–12954.
- Fischer, T.; Chang, H. J.; and Demiris, Y. 2018. Rt-gene: Real-time eye gaze estimation in natural environments. In *Proceedings of the European conference on computer vision (ECCV)*, 334–352.
- Ghosh, A.; Dabral, R.; Golyanik, V.; Theobalt, C.; and Slusallek, P. 2023. IMos: Intent-Driven Full-Body Motion Synthesis for Human-Object Interactions. *arXiv:2212.07555*.
- Gottlieb, J.; Oudeyer, P.-Y.; Lopes, M.; and Baranes, A. 2013. Information-seeking, curiosity, and attention: computational and neural mechanisms. *Trends in cognitive sciences*, 17(11): 585–593.
- Grady, P.; Tang, C.; Twigg, C. D.; Vo, M.; Brahmabhatt, S.; and Kemp, C. C. 2021. Contactopt: Optimizing contact to improve grasps. In *Proceedings of the IEEE/CVF Conference on Computer Vision and Pattern Recognition*, 1471–1481.
- Guan, Y.; Chen, Z.; Zeng, W.; Cao, Z.; and Xiao, Y. 2023. End-to-End Video Gaze Estimation via Capturing Head-Face-Eye Spatial-Temporal Interaction Context. *IEEE Signal Processing Letters*, 30: 1687–1691.
- Hampali, S.; Rad, M.; Oberweger, M.; and Lepetit, V. 2020. HOannotate: A Method for 3D Annotation of Hand and Object Poses. In *Proceedings of the IEEE/CVF Conference on Computer Vision and Pattern Recognition (CVPR)*.
- Jiang, H.; Liu, S.; Wang, J.; and Wang, X. 2021. Hand-object contact consistency reasoning for human grasps generation. In *Proceedings of the IEEE/CVF International Conference on Computer Vision*, 11107–11116.
- Karunratanakul, K.; Preechakul, K.; Suwajanakorn, S.; and Tang, S. 2023. Guided Motion Diffusion for Controllable Human Motion Synthesis. In *Proceedings of the IEEE/CVF International Conference on Computer Vision*, 2151–2162.
- Kothari, R.; De Mello, S.; Iqbal, U.; Byeon, W.; Park, S.; and Kautz, J. 2021. Weakly-supervised physically unconstrained gaze estimation. In *Proceedings of the IEEE/CVF Conference on Computer Vision and Pattern Recognition*, 9980–9989.
- Kratzer, P.; Bihlmaier, S.; Midlagajni, N. B.; Prakash, R.; Toussaint, M.; and Mainprice, J. 2020. Mogaze: A dataset of full-body motions that includes workspace geometry and eye-gaze. *IEEE Robotics and Automation Letters*, 6(2): 367–373.
- Kwon, T.; Tekin, B.; Stühmer, J.; Bogo, F.; and Pollefeys, M. 2021. H2O: Two Hands Manipulating Objects for First Person Interaction Recognition. In *Proceedings of the IEEE/CVF International Conference on Computer Vision (ICCV)*, 10138–10148.
- Li, H.; Lin, X.; Zhou, Y.; Li, X.; Huo, Y.; Chen, J.; and Ye, Q. 2022. Contact2Grasp: 3D Grasp Synthesis via Hand-Object Contact Constraint. *arXiv preprint arXiv:2210.09245*.
- Li, J.; Wu, J.; and Liu, C. K. 2023. Object motion guided human motion synthesis. *ACM Transactions on Graphics (TOG)*, 42(6): 1–11.
- Liu, M.; Tang, S.; Li, Y.; and Rehg, J. M. 2020. Forecasting human-object interaction: joint prediction of motor attention and actions in first person video. In *Computer Vision—ECCV 2020: 16th European Conference, Glasgow, UK, August 23–28, 2020, Proceedings, Part I 16*, 704–721. Springer.
- Liu, S.; Zhou, Y.; Yang, J.; Gupta, S.; and Wang, S. 2023. ContactGen: Generative Contact Modeling for Grasp Generation. In *Proceedings of the IEEE/CVF International Conference on Computer Vision*, 20609–20620.
- Liu, Y.; Liu, Y.; Jiang, C.; Lyu, K.; Wan, W.; Shen, H.; Liang, B.; Fu, Z.; Wang, H.; and Yi, L. 2022. HOI4D: A 4D Egocentric Dataset for Category-Level Human-Object Interaction. In *Proceedings of the IEEE/CVF Conference on Computer Vision and Pattern Recognition (CVPR)*, 21013–21022.



- Liu, Y.; Yang, H.; Si, X.; Liu, L.; Li, Z.; Zhang, Y.; Liu, Y.; and Yi, L. 2024. TACO: Benchmarking Generalizable Bimanual Tool-ACTION-Object Understanding. *arXiv preprint arXiv:2401.08399*.
- Lugaresi, C.; Tang, J.; Nash, H.; McClanahan, C.; Uboweja, E.; Hays, M.; Zhang, F.; Chang, C.; Yong, M. G.; Lee, J.; Chang, W.; Hua, W.; Georg, M.; and Grundmann, M. 2019. MediaPipe: A Framework for Building Perception Pipelines. *CoRR*, abs/1906.08172.
- Qi, C. R.; Yi, L.; Su, H.; and Guibas, L. J. 2017. Pointnet++: Deep hierarchical feature learning on point sets in a metric space. *Advances in neural information processing systems*, 30.
- Ragusa, F.; Furnari, A.; Livatino, S.; and Farinella, G. M. 2021. The meccano dataset: Understanding human-object interactions from egocentric videos in an industrial-like domain. In *Proceedings of the IEEE/CVF Winter Conference on Applications of Computer Vision*, 1569–1578.
- Romero, J.; Tzionas, D.; and Black, M. J. 2017. Embodied Hands: Modeling and Capturing Hands and Bodies Together. *ACM Transactions on Graphics, (Proc. SIGGRAPH Asia)*, 36(6).
- Schneider, W. X. 1995. VAM: A neuro-cognitive model for visual attention control of segmentation, object recognition, and space-based motor action. *Visual Cognition*, 2(2-3): 331–376.
- Seshan, A. 2022. Using Machine Learning to Augment Dynamic Time Warping Based Signal Classification. *arXiv preprint arXiv:2206.07200*.
- Taheri, O.; Choutas, V.; Black, M. J.; and Tzionas, D. 2022. GOAL: Generating 4D whole-body motion for hand-object grasping. In *Proceedings of the IEEE/CVF Conference on Computer Vision and Pattern Recognition*, 13263–13273.
- Taheri, O.; Zhou, Y.; Tzionas, D.; Zhou, Y.; Ceylan, D.; Pirk, S.; and Black, M. J. 2024. GRIP: Generating interaction poses using spatial cues and latent consistency. In *2024 International Conference on 3D Vision (3DV)*, 933–943. IEEE.
- Tevet, G.; Raab, S.; Gordon, B.; Shafir, Y.; Cohen-Or, D.; and Bermano, A. H. 2022. Human motion diffusion model. *arXiv preprint arXiv:2209.14916*.
- Yang, L.; Ding, S.; Cai, Y.; Yu, J.; Wang, J.; and Shi, Y. 2024. Guidance with Spherical Gaussian Constraint for Conditional Diffusion. *arXiv preprint arXiv:2402.03201*.
- Yang, L.; Li, K.; Zhan, X.; Wu, F.; Xu, A.; Liu, L.; and Lu, C. 2022. OakInk: A Large-Scale Knowledge Repository for Understanding Hand-Object Interaction. In *Proceedings of the IEEE/CVF Conference on Computer Vision and Pattern Recognition (CVPR)*, 20953–20962.
- Zhan, X.; Yang, L.; Zhao, Y.; Mao, K.; Xu, H.; Lin, Z.; Li, K.; and Lu, C. 2024. OAKINK2: A Dataset of Bimanual Hands-Object Manipulation in Complex Task Completion. In *Proceedings of the IEEE/CVF Conference on Computer Vision and Pattern Recognition*, 445–456.
- Zhang, H.; Ye, Y.; Shiratori, T.; and Komura, T. 2021. Manipnet: neural manipulation synthesis with a hand-object spatial representation. *ACM Transactions on Graphics (ToG)*, 40(4): 1–14.
- Zhang, J.; Luo, H.; Yang, H.; Xu, X.; Wu, Q.; Shi, Y.; Yu, J.; Xu, L.; and Wang, J. 2023. NeuralDome: A Neural Modeling Pipeline on Multi-View Human-Object Interactions. In *Proceedings of the IEEE/CVF Conference on Computer Vision and Pattern Recognition (CVPR)*, 8834–8845.
- Zhao, C.; Zhang, J.; Du, J.; Shan, Z.; Wang, J.; Yu, J.; Wang, J.; and Xu, L. 2023. I<sup>2</sup>M HOI: Inertia-aware Monocular Capture of 3D Human-Object Interactions. *arXiv preprint arXiv:2312.08869*.
- Zheng, J.; Zheng, Q.; Fang, L.; Liu, Y.; and Yi, L. 2023. CAMS: CANonicalized Manipulation Spaces for Category-Level Functional Hand-Object Manipulation Synthesis. In *Proceedings of the IEEE/CVF Conference on Computer Vision and Pattern Recognition*, 585–594.
- Zheng, Y.; Yang, Y.; Mo, K.; Li, J.; Yu, T.; Liu, Y.; Liu, C. K.; and Guibas, L. J. 2022. Gimo: Gaze-informed human motion prediction in context. In *European Conference on Computer Vision*, 676–694. Springer.
- Zhou, K.; Bhatnagar, B. L.; Lenssen, J. E.; and Pons-Moll, G. 2024. GEARS: Local Geometry-aware Hand-object Interaction Synthesis. In *Proceedings of the IEEE/CVF Conference on Computer Vision and Pattern Recognition*, 20634–20643.